ChemSystemsChem

Research Article
doi.org/10.1002/syst.202200027

Chemistry Europe
European Chemical Societies Publishing

www.chemsystemschem.org

Check for updates

Special Collection

Generation of Bilayer Asymmetry and Membrane Curvature by the Sugar-Cleaving Enzyme Invertase

Abhimanyu Nowbagh,[a] Akshi Deshwal,[b] Mayur Kadu,[a] Abhishek Chaudhuri,[a] Subhabrata Maiti,[b] Reinhard Lipowsky,*[c] and Tripta Bhatia*[a]

The catalytic action of invertase generates bilayer asymmetry that stabilises membrane curvature. The driving mechanism for the generation of membrane curvature by invertase is investigated using giant unilamellar vesicles (GUVs). The invertase cleaves the sucrose in the exterior compartment, thereby creating a sugar asymmetry across the bilayer membrane that is measured for GUV membranes consisting of the lipid Dioleoylphosphatidylcholine (DOPC). Finally, the advantage of this method to control membrane curvature and to stabilize multisphere morphologies is demonstrated. The GUV system in the presence of invertase is beneficial as a tool to generate multiple on-demand compartments with more extended stability after the enzymatic activity has established the asymmetry.

Introduction

Directional bending of cellular biomembranes remains a highly active research area because of its importance for various cellular pathways.[1–4] Membrane bending is observed in many cell-biological processes and often involves membrane proteins. The plasma membrane, for instance, consists of an asymmetric lipid-protein bilayer which bends outward or inward depending on the direction in which mass or information transfer is required for the cell. In this paper, we discuss the generation of membrane curvature of cell-sized, protein-free lipid membrane compartments, namely giant unilamellar vesicles (GUVs)[5] exposed to millimolar sucrose solutions and a nanomolar solution of the sugar-cleaving enzyme[6–10] invertase in the exterior solution.[4,11]

Compositional asymmetry arising from different lipid compositions in the two leaflets of the bilayer membrane has been studied for some time.[12,13] In general, a transbilayer asymmetry between the two leaflets can be generated by many different molecular mechanisms.[5] Here, we consider the asymmetry arising from adsorption/depletion layers of sugar molecules which are formed in close proximity to the two leaflets[14,15] and lead to different molecular interactions of the two leaflets with the adjacent aqueous solutions.

The GUVs are composed of the lipid Dioleoylphosphatidylcholine (DOPC) in the fluid phase prepared in a 300 mM sucrose solution (see Methods in SI). The image in Figure 1a displays a quasi-spherical GUV observed under the phase-contrast microscope. This GUV is in contact with 300 mM sucrose solution in the interior and exterior solution. Using phase-contrast microscopy, one observes a sharp membrane boundary because of the refractive index mismatch between the lipid bilayer and the sucrose solution. The vesicle size R_{ve} is obtained from the measured surface area A of the membrane [Eq. (1)].

$$R_{ve} \equiv \sqrt{A/4\pi} \tag{1}$$

The measured vesicle volume V and the surface area A defines the volume-to-area ratio v [Eq. (2)].

$$v \equiv 3V/4\pi R_{ve}^3 \tag{2}$$

Figure 1b shows the same GUV after one minute of adding the invertase to the bulk solution (outside the GUVs). Time-

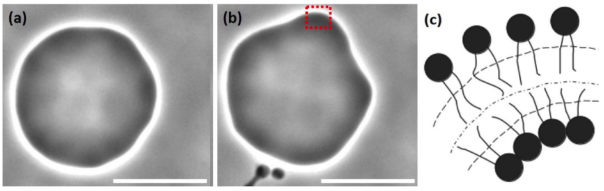

Figure 1. Membrane deformation of a GUV in about a minute. (a,b) Shape changes of a GUV from quasi-spherical to non-spherical shape in the presence of the enzyme invertase in the bulk solution as observed by phase-contrast microscopy. A small region of the GUV membrane is highlighted by the red box in Figure 1b. (c) Expansion and compression of outer and inner bilayer leaflet shown schematically for a small outward bulged region of the GUV membrane corresponding to the red box in (b). The black balls represent the head group, and the two continuous lines represent the tails. Scale bars: 10 μm.

[a] A. Nowbagh, M. Kadu, Dr. A. Chaudhuri, Dr. T. Bhatia
Department of Physical Sciences, Indian Institute of Science Education and Research (IISER) Mohali, Knowledge City, Manauli 140306, India
E-mail: triptabhatia@iisermohali.ac.in
[b] A. Deshwal, Dr. S. Maiti
Department of Chemical Sciences, Indian Institute of Science Education and Research (IISER) Mohali, Knowledge City, Manauli 140306, India
[c] Prof. Dr. R. Lipowsky
Max Planck Institute of Colloids and Interfaces, Science Park Golm, 14424 Potsdam, Germany
E-mail: lipowsky@mpikg.mpg.de

Special Collection An invited contribution to a Special Collection on Protocells and Prebiotic Systems

© 2022 The Authors. ChemSystemsChem published by Wiley-VCH GmbH. This is an open access article under the terms of the Creative Commons Attribution Non-Commercial License, which permits use, distribution and reproduction in any medium, provided the original work is properly cited and is not used for commercial purposes.

© 2022 The Authors. ChemSystemsChem published by Wiley-VCH GmbH

25704206, 2023, 2, Downloaded from https://chemistry-europe.onlinelibrary.wiley.com/doi/10.1002/syst.202200027 by Max-Planck-Institut Fur Kolloi, Wiley Online Library on [14/03/2023]. See the Terms and Conditions (https://onlinelibrary.wiley.com/terms-and-conditions) on Wiley Online Library for rules of use; OA articles are governed by the applicable Creative Commons License

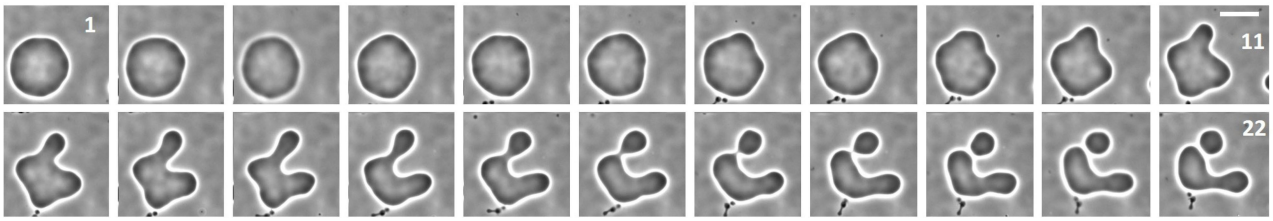

Figure 2. Generation of membrane curvature by invertase. The first frame ($t=0$), shows a quasi-spherical GUV with 300 mM sucrose solution inside and in the exterior. Invertase is added at $t=0$. Shape changes as observed by phase-contrast microscopy, evolving from the beginning towards the eleventh frame ($t\sim97$ s) and the twenty-second frame ($t\sim203$ s) are indicated. The two consecutive frames are separated by about 9.675 s. The buds remain connected to the mother GUV by a narrow membrane neck. The scale bar in the frame eleventh is 10 μm and applies to all frames.

lapse images of the same GUV up to about 200 s are shown in Figure 2, where frame 1 is the same as Figure 1a. As we move from frame 1 to frame 22 in Figure 2, the concentration of fructose and glucose in bulk increases with time at the expense of a decreasing concentration of sucrose by the action of the enzyme shown in Figure 3. Invertase splits one sucrose molecule to one fructose and one glucose molecule. Now, for an outward bending of the GUV membrane shown in Figure 1b and Figure 2, the outer and the inner leaflets of the bilayer undergo expansion and compression,[16] respectively, relative to the mid surface shown in Figure 1c. The black balls schematically represent the head groups of the lipid molecules and the two continuous lines represent the lipid tails. The view of the two bilayer leaflets as shown in Figure 1c was first emphasized by Evans.[17]

Previous studies suggested that small solutes such as sugars in contact with lipid membranes can generate membrane curvature by forming adsorption or depletion layers at the two sides of the bilayer membranes.[14,15,18–23] The formed multisphere compartments are continuous, connected by membrane necks and can encapsulate chemicals of interest. The generation of membrane curvature and compartments has many potential applications in the pharmaceutics and applied biochemistry for drug delivery, where GUVs act as a carrier for entrapped drugs.[24]

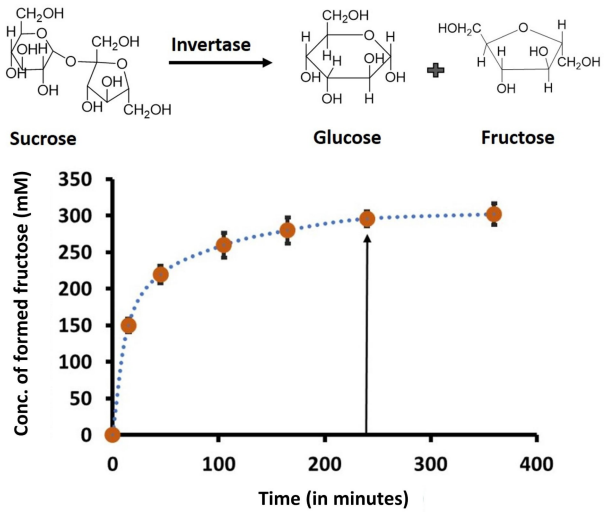

Figure 3. Conversion of one sucrose molecule to one molecule of fructose and one molecule of glucose by the enzyme invertase. The experimental plot shows the concentration of the liberated fructose as a function of time. Initial concentration of sucrose is 300 mM and of Invertase is 50 nM. The experimental details are given in Figure S2. After 2 hours, almost 90% of the sucrose molecules have been converted. The arrow is pointing at the 4 hour mark, showing a complete conversion of 300 mM sucrose to 300 mM fructose and 300 mM glucose.

Results and Discussion

We discuss the invertase-induced generation of bilayer curvature arising from asymmetric adsorption or depletion layers at the two bilayer leaflets.[14,18] Small-angle neutron scattering and thermodynamic measurements[20] demonstrated adsorption and depletion of sugar molecules at the two leaflets of a lipid bilayer. In the present study, the inner leaflet is always in contact with sucrose whereas the outer leaflet is exposed to a solution of sucrose as well as glucose and fructose, resulting from the enzymatic conversion of sucrose into glucose and fructose by invertase, see Figure 3.

The GUVs are prepared in 300 mM sucrose. We then add 50 nM invertase to the exterior solution and monitor the sucrose conversion by high-performance liquid chromatography (HPLC), see Figures S1 and S2 of the Supplementary Information (SI). In about 4 hours, the 300 mM sucrose solution is completely converted into an equimolar solution of 300 mM fructose and 300 mM glucose as shown in Figure 3. This implies that, after 4 hours, the total sugar concentration in the exterior solution has reached an increased value that is close to 600 mM. A similar conversion has been reported previously.[4]

Sucrose, glucose and fructose cannot cross the GUV membranes. Therefore, the osmotic imbalance generated by the enzyme is compensated by permeation of water from the interior solutions of the GUVs to the exterior solution, thereby deflating the GUVs and increasing the sucrose concentration in the interior solutions. After 4 hours, both the interior and the exterior solutions have reached the same sugar concentration close to 600 mM.

© 2022 The Authors. ChemSystemsChem published by Wiley-VCH GmbH

25704206, 2023, 2, Downloaded from https://chemistry-europe.onlinelibrary.wiley.com/doi/10.1002/syst.202200027 by Max-Planck-Institut Fur Kolloi, Wiley Online Library on [14/03/2023]. See the Terms and Conditions (https://onlinelibrary.wiley.com/terms-and-conditions) on Wiley Online Library for rules of use; OA articles are governed by the applicable Creative Commons License

Generation of bilayer asymmetry by invertase

In frame 1 of Figure 2, the outer and inner leaflets of the bilayer are in contact with a 300 mM sucrose solution. In frame 22 ($t \sim 203$ s) of Figure 2, the outer leaflet is in contact with a mixture of sucrose, fructose and glucose, as follows from Figure 3, whereas the inner leaflet remains in contact with sucrose. After about 4 hours, the inner leaflet is still exposed to only sucrose but the outer leaflet is now exposed to 50% glucose and 50% fructose. Therefore, during the time course of 4 hours after adding the invertase, the inner leaflet experiences a time-dependent variation of sugar concentration at a constant sugar composition. In contrast, the outer leaflet experiences a time-dependent variation of both sugar composition and sugar concentration.

Generation of GUV membrane curvature

The morphological shape changes of the GUV shown in Figure 2 imply that invertase can generate membrane curvature in the outward direction. We analyse the GUV shapes after 4 hours, to estimate the spontaneous curvature of the GUV membrane in equilibrium. In our previous study,[15] the GUV membranes contained cholesterol which undergoes frequent flip-flops between the leaflets. The resulting morphologies were quantitatively described by the spontaneous curvature model.[25,26] In the present study, the bilayers consist of a single phospholipid that hardly undergoes flip-flops from one leaflet to the other. Therefore, each leaflet contains a conserved number of lipids as described by area-difference elasticity (ADE).[27–29] As a consequence, the spontaneous curvature m considered here can be decomposed into two parts,[28,30] a local part that has the same form as in the spontaneous curvature model and a non local part arising from the ADE constraint.

The spontaneous curvature gives a quantitative estimate of the bilayer asymmetry. Because the GUV membrane bulged outward, the GUV membranes studied here have a positive, spontaneous curvature. We observed many different multi-sphere morphologies of GUVs in the experiments. We have selected carefully those GUVs with multiple quasi-spherical membrane segments that remain well in focus and exhibit stably closed membrane necks during the optical imaging. The phase-contrast is maximum if and only if the membrane segments are quasi-spherical and have the maximum contrast at their equatorial plane, providing a precise estimate of their diameter. These membrane segments have their largest cross-sections, almost circular to an excellent approximation. For sucrose in the interior and fructose and glucose in the exterior compartment, this selection criterion led to the 14 GUVs discussed in Table S1.

Figure 4 shows three spheres connected by two membrane necks forming three different patterns. The neck mean curvature $M_{ne} \equiv M_{ab}$ of an ab-neck Eq. (3), between two spheres a and b is defined by[2,15]

$$M_{ab} = \frac{1}{2}\left[\frac{1}{R_a} + \frac{1}{R_b}\right] \tag{3}$$

where $1/R_a$ and $1/R_b$ are the mean-curvatures of the two spheres a and b. The membrane ab-neck remains stably closed if $m \geq M_{ab}$ but opens up for $m < M_{ab}$.[2,15] In addition to their stability against neck opening, multispherical shapes must also be stable against prolate deformations of the individual spheres. The latter stability criterion leads to an upper bound, B_{up}, for the spontaneous curvature.[15] Thus, for each individual GUV, we obtain two inequalities for the spontaneous curvature m as given by Eq. (4).

$$M_{ab} \leq m < B_{up} \equiv \frac{3}{R_s(1 - R_s/R_l)} \tag{4}$$

As mentioned, the spontaneous curvature m considered here has a local and a nonlocal part,[28,30] as described by the spontaneous curvature model and the ADE constraint, respectively.

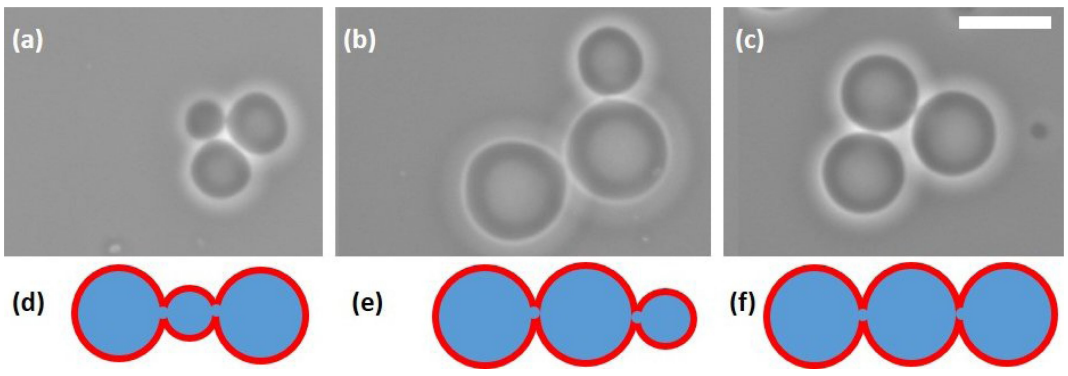

Figure 4. Three-sphere morphologies of GUVs generated by 50 nM invertase after 4 hours: (a,d) The small sphere is located between the two large spheres. (b,e) The small sphere is at the end of a necklace with two large spheres. (c,f) The three spheres have equal sizes. The scale bar is 10 μm. The time of imaging is 4 hours after the enzyme incubation. (d–f) Schematics for the images. Red colour is used for the GUV membrane, blue for the sucrose solution in the interior of the GUV. The sugar concentration is close to 600 mM with sucrose in the interior and an equimolar mixture of fructose and glucose in the exterior solution. The scale bar in (c) is 10 μm and applies to panels (a-c).

© 2022 The Authors. ChemSystemsChem published by Wiley-VCH GmbH

25704206, 2023, 2, Downloaded from https://chemistry-europe.onlinelibrary.wiley.com/doi/10.1002/syst.202200027 by Max-Planck-Institut Fur Kolloi, Wiley Online Library on [14/03/2023]. See the Terms and Conditions (https://onlinelibrary.wiley.com/terms-and-conditions) on Wiley Online Library for rules of use; OA articles are governed by the applicable Creative Commons License

The multispheres in Figure 4a-c consist of small and large spheres that form different patterns. The small sphere in Figure 4a is in-between two large spheres whereas the small sphere in Figure 4b is connected to only one large sphere. Figure 4c displays a necklace with three equally sized spheres. The patterns corresponding to the images in Figures 4a-c are shown schematically in Figures 4d–f. The different patterns involve different types of necks with different neck curvatures. The mean curvature of membrane necks[2,15] connecting one large and one small spheres as in Figures 4a and b is equal to $M_{ls} = \frac{1}{2}\left(R_l^{-1} + R_s^{-1}\right)$ as follows from Eq. (3) for $a = l$ and $b = s$. The sphere pattern in Figure 4b also involves a neck between two large spheres. The corresponding neck mean curvature is equal to $M_{ll} = 1/R_l$ as obtained from Eq. (3) for $a = b = l$. Finally, the multisphere in Figure 4c involves two membrane necks between three equally sized spheres of radius $R*$. The mean curvature of such a membrane neck is equal to $M* = 1/R*$, corresponding to Eq. (3) with $a = b =$*.

We now analyze the inequalities in Eq. (4) for 14 GUVs which were selected from a single batch of vesicles. For each of these GUVs, the neck mean curvature M_{ne} and the upper bound B_{up}, as defined in Eqs. (3) and (4), were determined from the optical images. The numerical values of these two geometric quantities are given in Table S1 and used for the analysis in Figure 5. In this way, we obtain 14 lower and 14 upper bounds for the spontaneous curvature m. Because all 14 GUVs have been prepared in the same way, both leaflets of these GUVs are exposed to the same total sugar concentration of close to 600 mM, with the inner and outer leaflets being exposed to sucrose and an equimolar mixture of fructose and glucose, respectively. Therefore, the bilayer membranes of all 14 GUVs should possess the same spontaneous curvature. In order to improve the inequalities in Eq. (4), we now choose the largest value of the lower bound M_{ne} and the smallest value of the upper bound B_{up}. The largest value of M_{ne} is $(0.25\pm0.01)\mu m^{-1}$, corresponding to the GUV with index number 2 in Figure 5. The smallest value of B_{up} is $(1.07\pm0.05)\mu m^{-1}$, corresponding to the GUV with index number 9 in Figure 5. Therefore, we obtain the improved bounds $0.25\,\mu m^{-1} \leq m \leq 1.07\,\mu m^{-1}$ which lead to the estimate $m = \frac{1}{2}(0.25 + 1.07)\,\mu m^{-1} = (0.66 \pm 0.4)\,\mu m^{-1}$ for the spontaneous curvature. This spontaneous curvature value is smaller than the one deduced in our previous study[15] on GUV membranes with cholesterol, which undergoes frequent flip-flops. In the latter case, the ADE constraint is absent and the spontaneous curvature has only a local part as described by the spontaneous curvature model. In contrast, the GUV membranes studied here contain no cholesterol which leads to a nonlocal part of the spontaneous curvature. This nonlocal part is typically negative[30] which explains the reduced value of m obtained here.

Using invertase-free control experiments, we have checked that the sugar asymmetry is indeed responsible for generating membrane curvature as demonstrated in Figures S3 and S4 of the SI. We prepared GUVs of DOPC encapsulating a sucrose solution of 300 mM and transferred these GUVs into the observation chamber filled with an equimolar mixture of 300 mM fructose and 300 mM glucose. The resulting values for the neck mean curvatures M_{ne} and the upper bounds B_{up} are displayed in Figure S4. Inspection of this figure shows that the largest value of M_{ne} is now equal to $(0.25\pm0.00)\,\mu m^{-1}$, corresponding to the GUV with index number 11 whereas the smallest value of B_{up} is $(0.92\pm0.01)\mu m^{-1}$ for the GUV with index number 7. Therefore, we obtain the improved bounds $0.25\,\mu m^{-1} \leq m \leq 0.92\,\mu m^{-1}$ for the spontaneous curvature m which lead to the estimate $m = \frac{1}{2}(0.25 + 0.92)\,\mu m^{-1} = (0.59 \pm 0.33)\,\mu m^{-1}$. In addition, as described in the SI, control experiments with tagged invertase[31] were carried out to confirm that invertase does not directly bind to the GUV membranes.

Conclusion

We have used the catalytic sugar-cleaving ability of invertase to generate bilayer asymmetry that stabilises membrane curvature. After 4 hours, both leaflets of the GUV membranes are exposed to the same total sugar concentration, which is close to 600 mM, with the inner and outer leaflets being exposed to sucrose and an equimolar mixture of fructose and glucose, respectively. Using control experiments (Figs S3 and S4), we have checked that this sugar asymmetry between sucrose and fructose plus glucose is indeed responsible for generating the membrane curvature. Compared to sucrose, glucose and fructose have additional chemical groups that can interact with

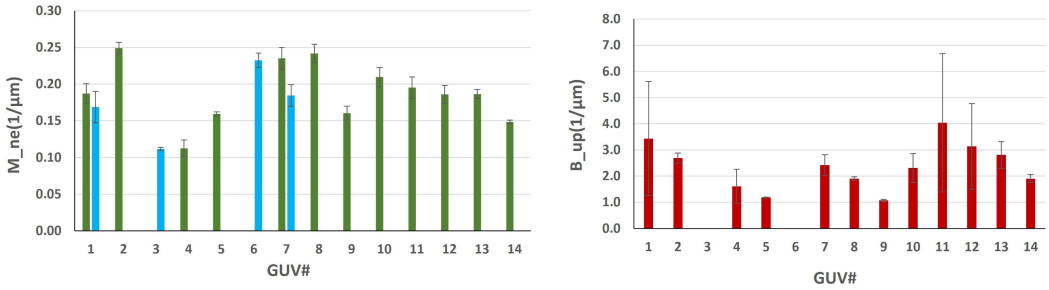

Figure 5. The neck curvature M_{ne} and the upper curvature bound B_{up} for 14 GUVs exposed to invertase. The green color is for M_{ls} and the blue color is for M_{ll}. The values of the shape parameters are provided in Table S2. The neck curvature varies between $(0.111 \pm 0.002)\mu m^{-1}$ and $(0.249 \pm 0.008)\mu m^{-1}$. The value of the upper curvature bound B_{up} is varying between $(1.071 \pm 0.045)\mu m^{-1}$ and $(4.037 \pm 2.642)\mu m^{-1}$.

© 2022 The Authors. ChemSystemsChem published by Wiley-VCH GmbH

25704206, 2023, 2, Downloaded from https://chemistry-europe.onlinelibrary.wiley.com/doi/10.1002/syst.202200027 by Max-Planck-Institut Fur Kolloi, Wiley Online Library on [14/03/2023]. See the Terms and Conditions (https://onlinelibrary.wiley.com/terms-and-conditions) on Wiley Online Library for rules of use; OA articles are governed by the applicable Creative Commons License

the lipids. Second, glucose and fructose are both smaller than sucrose. Therefore, glucose and fructose can form more densely packed adsorption layers at the outer leaflets. In summary, we have demonstrated that the transbilayer asymmetry arising from different carbohydrates, such as sucrose, glucose and fructose, creates membrane curvature of GUV membranes. This curvature generation can be induced by using the catalytic activity of the sugar-cleaving enzyme invertase, starting from symmetric bilayer membranes. Future studies will extend our approach by varying the initial sugar concentration in the exterior solution which determines the final sugar asymmetry and spontaneous curvature as well as the enzyme concentration which modifies the speed by which this sugar asymmetry can be achieved. Another challenge for future studies is to divide the multispherical GUVs described here into several membrane compartments by increasing the spontaneous curvature, thereby cleaving the membrane necks.[32]

Author Contribution

TB designed the experiments, RL developed the theory. AN, AD, MK, and TB performed experiments and controls. AD and SM did invertase tagging and HPLC measurements. AN, TB, and RL analyzed the data and fitted them to theoretical models. TB and RL wrote the manuscript. All authors discussed the manuscript and commented on it.

Acknowledgements

This research was conducted within the Indian Institute of Science Education and Research Mohali and supported by the Ramalingaswami grant of DBT (grant BT/RLF/Re-entry/06/2020). The Max Planck Society provides open access funding. Open Access funding enabled and organized by Projekt DEAL.

Conflict of Interest

The authors declare no conflict of interest.

Data Availability Statement

The data that support the findings of this study are available in the supplementary material of this article.

Keywords: Invertase · Membrane curvature · Giant unilamellar vesicle · Bilayer asymmetry · Hydrolysis

[1] I. K. Jarsch, F. Daste, L. Gallop, *J. Cell Biol.* **2016**, *214*, 375.
[2] R. Lipowsky, *Adv. Biology* **2022**, *6*, 2101020.
[3] S. F. Fenz, K. Sengupta, *Integr. Biol.* **2012**, *4*, 1757.
[4] Y. Dreher, K. Jahnke, E. Bobkova, J. P. Spatz, K. Göpfrich, *Angew. Chem. Int. Ed.* **2021**, *60*, 10661–10669.
[5] R. Dimova, C. M. Marques (Editors), *The Giant Vesicle Book*, Springer Verlag **2019**.
[6] S. M. Kotwal, V. Shankar, *Biotechnol. Adv.* **2009**, *27*, 311–322.
[7] Y. Ruana, Y. Jin, Y. Yang, G. Li, J. S. Boyere, *Molecular Plant* **2010**, *3*, 942–955.
[8] H. Winter, S. C. Huber, *CRC Crit Rev Plant Sci* **2010**, *19*, 31–67.
[9] S. Kulshrestha, P. Tyagi, V. Sindhi, K. S. Yadavilli, *J. Pharm. Res.* **2013**, *7*, 792–797.
[10] J. Verbančič, J. E. Lunn, M. Stitt, S. Persson *Molecular Plant* **2018**, *11*, 75–94.
[11] J. H. Koschwanez, K. R. Foster, A. W. Murray, *PLoS Biol.* **2011**, *9*, e1001122.
[12] J. E. Rothman, J. Lenard, *Science* **1977**, *195*, 743–753.
[13] J. E. Rothman, *Sci. Am.* **1979**, *240*, 48–63.
[14] R. Lipowsky, H. G. Döbereiner, *Europhys. Lett.* **1998**, *43*, 219.
[15] T. Bhatia, S. Christ, J. Steinkühler, R. Dimova, R. Lipowsky, *Soft Matter* **2020**, *16*, 1246.
[16] U. Seifert, S. A. Langer, *Europhys. Lett.* **1993**, *23*, 71.
[17] E. Evans, *Biophys. J.* **1974**, *14*, 923.
[18] R. Lipowsky, *Adv. Colloid Interface Sci.* **2022**, *301*, 102613.
[19] P. Westh, *Phys. Chem. Chem. Phys.* **2008**, *10*, 4110.
[20] H. D. Andersen, C. H. Wang, L. Arleth, G. H. Peters, P. Westh, *Proc. Natl. Acad. Sci. USA* **2011**, *108*, 1874.
[21] G. V. D. Bogaart, N. Hermans, V. Krasnikov, A. H. D. Vries, B. Poolman, *Biophys. J.* **2007**, *92*, 1598.
[22] V. Vitkova, J. Genova, M. D. Mitov, I. Bivas, *Mol. Cryst. Liq. Cryst.* **2006**, *449*, 95.
[23] T. Bhatia, *J. Membr. Biol.* **2022**, DOI: 10.1007/s00232-022-00254-w.
[24] T. Noyhouzer, C. L'Homme, I. Beaulieu, S. Mazurkiewicz, S. Kuss, H. Kraatz, S. Canesi, J. Mauzeroll, *Langmuir* **2016**, *32*, 4169.
[25] W. Helfrich, *Z. Naturforsch. C* **1973**, *28*, 693.
[26] U. Seifert, K. Berndl, R. Lipowsky, *Phys. Rev. A* **1991**, *44*, 1182.
[27] U. Seifert, L. Miao, H. G. Döbereiner, M. Wortis, *The structure and conformation of amphiphilic membranes*, volume 66, Springer, Berlin, Heidelberg **1992**.
[28] H. G. Döbereiner, E. Evans, M. Kraus, U. Seifert, M. Wortis, *Phys. Rev. E* **1997**, *55*, 4458.
[29] S. Svetina, B. Zeks, *Anat. Rec.* **2002**, *268*, 215.
[30] R. Lipowsky, *The Giant Vesicle Book*, Chapter 5, Springer Verlag **2019**, page 73.
[31] S. Rani, B. Dasgupta, G. K. Bhati, K. Tomar, S. Rakshit, S. Maiti, *ChemBioChem* **2020**, *22*, 1285–1291.
[32] J. Steinkühler, R. L. Knorr, Z. Zhao, T. Bhatia, S. M. Bartelt, S. Wegner, R. Dimova, R. Lipowsky, *Nat. Commun.* **2020**, *11*, 905.

Manuscript received: July 30, 2022
Accepted manuscript online: November 7, 2022
Version of record online: December 7, 2022

© 2022 The Authors. ChemSystemsChem published by Wiley-VCH GmbH

25704206, 2023, 2, Downloaded from https://chemistry-europe.onlinelibrary.wiley.com/doi/10.1002/syst.202200027 by Max-Planck-Institut Fur Kolloi, Wiley Online Library on [14/03/2023]. See the Terms and Conditions (https://onlinelibrary.wiley.com/terms-and-conditions) on Wiley Online Library for rules of use; OA articles are governed by the applicable Creative Commons License